The EMBO Journal vol.10 no.9 pp.2331 - 2341, 1991

Three-dimensional structure of a mouse-adapted type 2/type 1 poliovirus chimera

T.O.Yeates[1,4], D.H.Jacobson[1,3], A.Martin[2], C.Wychowski[2], M.Girard[2], D.J.Filman[1,3] and J.M.Hogle[1,3]

[1]Department of Molecular Biology, Research Institute of Scripps Clinic, 10666 North Torrey Pines Road, La Jolla, CA 92037, USA and [2]Pasteur Institute, Virologie Moleculaire, 25 rue du Dr Roux, 75724 Cedex 15 Paris, France

Present addresses: [3]Department of Biological Chemistry and Molecular Pharmacology, Harvard Medical School, 240 Longwood Avenue, Boston, MA 02115 and [4]Department of Chemistry and Biochemistry, University of California Los Angeles, 405 Hilgard Avenue, Los Angeles, CA 90024, USA

Communicated by M.Girard

The crystal structure of V510, a chimeric type 2/type 1 poliovirus, has been determined at 2.6 Å resolution. Unlike the parental Mahoney strain of type 1 poliovirus, V510 is able to replicate in the mouse central nervous system, due entirely to the replacement of six amino acids in the exposed BC loop of capsid protein VP1. Significant structural differences between the two strains cluster in a major antigenic site of the virus, located at the apex of the radial projection which surrounds the viral five-fold axis. Residues implicated in the mouse-virulence of poliovirus by genetic studies are located in this area, and include the residues which are responsible for stabilizing the conformation of the BC loop in V510. Despite evidence that this area is not involved in receptor binding in cultured primate cells, the genetic and structural observations suggest that this area plays a critical role in receptor interactions in the mouse central nervous system. These results provide a structural framework for further investigation of the molecular determinants of host and tissue tropism in viruses.

Key words: chimeric virus/host-range/neurovirulence/poliovirus/structure

Introduction

Site-specific modification of picornavirus genomes provides a powerful technique for defining the role of specific sequences in determining the biological properties of these viruses. Within the past three years several groups have reported the construction of chimeric polioviruses in which antigenic sites of type 1 poliovirus have been replaced by sequences from heterologous poliovirus serotypes or from heterologous viral or bacterial pathogens (Burke *et al.*, 1988; Colbere-Garapin *et al.*, 1988; Martin *et al.*, 1988; Murray *et al.*, 1988a,b; Evans *et al.*, 1989; Murdin and Wimmer, 1989; Jenkins *et al.*, 1990). The viability of the chimeras demonstrates that several loops exposed on the surface of poliovirus are able to accommodate a broad range of sequences, leading to the suggestion that chimeric polioviruses may be useful as novel vaccines (Burke *et al.*, 1988). Crystallographic study of these chimeras provides an opportunity to define the structural consequences of these substitutions and their effect on viral phenotype.

We report here the high-resolution structure of a type 2/type 1 poliovirus chimera, designated V510. V510 differs from its type 1 parent (P1/Mahoney) only in the replacement of a single external loop (the BC loop of capsid protein VP1, residues 94–102) by the corresponding residues from the Lansing strain of type 2 poliovirus (P2/Lansing). These residues constitute a major portion of antigenic site 1 of poliovirus (Minor *et al.*, 1986) and, as expected, the chimera is neutralized by anti-type 1 and anti-type 2 antibodies, and elicits a neutralizing response to both parental serotypes (Martin *et al.*, 1988). P2/Lansing is unusual in that it is able to cause paralysis upon direct intracerebral inoculation in mice, whereas most poliovirus strains (including P1/Mahoney) are specific for primates. V510 is of particular interest because replacement of the loop, corresponding to just six amino acid changes, has been shown to be sufficient to confer mouse-adaptation on the chimera (Martin *et al.*, 1988). Thus, V510 represents a simple model system for assessing the effects of amino acid substitutions and associated structural changes on the host range, tissue specificity and serotype specificity of poliovirus.

Poliovirus structure

The antigenic sites of all three serotypes of poliovirus have been well characterized (Minor *et al.*, 1986; Page *et al.*, 1988) and the three-dimensional structures of representative strains of types 1 and 3 poliovirus (P1/Mahoney and P3/Sabin, respectively) have been determined by X-ray crystallographic methods (Hogle *et al.*, 1985; Filman *et al.*, 1989). The poliovirus capsid is composed of 60 copies of each of four proteins, VP1, VP2, VP3 and VP4 (mol. wts 33 000, 30 000, 26 000 and 7500 respectively) arranged on a T = 1 icosahedral surface. Crystallographic studies of poliovirus [and of other members of the picornavirus family (Hogle *et al.*, 1985; Rossman *et al.*, 1985; Luo *et al.*, 1987; Acharya *et al.*, 1989; Filman *et al.*, 1989; Kim *et al.*, 1989)] have shown that the three large capsid proteins share a common core structural motif, an eight-stranded antiparallel β barrel (Figure 1a). In contrast to the structural conservation of the cores, the proteins have dissimilar extensions at their amino and carboxy termini, and dissimilar loops connecting the regular secondary-structural elements of the cores. In the virions the cores pack to form the closed shell of the capsid with the narrow ends of the cores of VP1 pointing towards the five-fold axes, and the narrow ends of the cores of VP2 and VP3 alternating around the three-fold axes of the particle (Figure 1b). The carboxy-terminal extensions and many of the connecting loops are located on the outer surface of the virion and form the neutralizing antigenic sites. Comparison of the structures of type 1 and type 3 poliovirus (Filman *et al.*, 1989) indicates that almost all significant structural differences between the two serotypes occur in

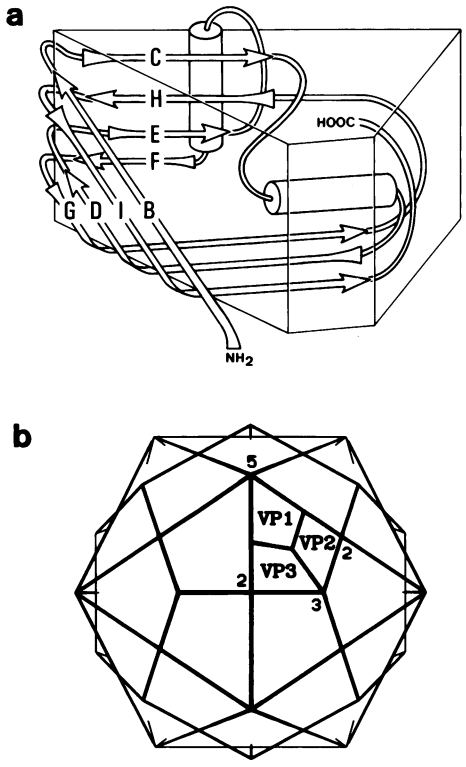

Fig. 1. The structure of the major capsid proteins of poliovirus and their organization in the virion. (**a**) A schematic representation of the conserved wedge-shaped eight-stranded antiparallel β barrel core motif shared by VP1, VP2 and VP3. Individual β strands are shown as arrows and are labeled alphabetically. Flanking helices are indicated by cylinders. (**b**) A geometric representation of the outer surface of the poliovirion generated by superimposing an icosahedron and a dodecahedron. The symmetry axes of the particle and the positions of VP1, VP2 and VP3 in one promoter are indicated. Like the virion, the geometric figure has large radial projections at the five-fold axes and somewhat smaller projections at the three-fold axes.

the antigenic sites. These structural differences generally correspond to the sites of insertions and deletions in the amino acid sequence, or to the replacement of prolines by non-prolines in regions containing several other sequence changes. The largest conformational difference (as much as 8 Å between equivalent α carbons) occurs in the BC loop of VP1 (residues 92–105) which is the site of substitution in the V510 chimera.

Results

A three-dimensional data set was constructed from 32 oscillation photographs (oscillation range 25′) obtained from five crystal. Statistics for the data are summarized in Table I. The structure was solved by molecular replacement, using an appropriately oriented and positioned refined model of P1/Mahoney to initiate phasing. Initial phase estimates were refined by the application of non-crystallographic symmetry constraints. Significant structural differences were confirmed using icosahedrally-constrained omit maps and difference maps (Figure 2). In addition to significant structural changes in the BC loop of VP1 (at residues 93–104), the resulting maps provided evidence for localized changes in the adjacent HI loop (residues 244–252) and an extensive conformational rearrangement in the nearby DE loop (residues 141–153). Two additional structural changes were identified at sites

Table I. Statistics for the V510 data set

Crystals (no.)	5
Films (no.)	32
Measurements (no.)	986739
Unique hkl measured (no.)	512096
Unique hkl used (no.)	437474
R_{sym} (all measurements >50% partial)	17.0%
R_{sym} (fully recorded reflections)	12.9%

R_{sym} compares multiply-measured individual partiality-corrected intensities (I_{hj}) with their statistically-weighted mean $<I_h>$.

$$R_{sym} = \frac{\sum_h \sum_j | I_{hj} - <I_h> |}{\sum_h \sum_j <I_h>} \times 100$$

distant from the substituted BC loop: a cation-binding site at the point at which the carboxy terminus of VP3 exits the core, and the lipid binding site in the middle of the VP1 β barrel. A complete atomic model which incorporates these changes was constructed to fit the density, and subsequently was refined using alternating cycles of pseudo-real space atomic refinement (Filman *et al.*, 1989), non-crystallographic averaging, and interactive model building. Statistics for the current refined model are presented in Table II. The co-ordinates for the current model will be deposited in the Brookhaven Protein Database.

Structural differences in the V510 chimera

As expected, the structure of the V510 chimera is very similar to that of P1/Mahoney. If the large localized structural changes in the BC and DE loops of VP1 are ignored, the root-mean-squared (r.m.s.) difference in the positions of equivalent atoms is only 0.21 Å. This is consistent with the expected level of random error in the two models. In contrast, differences between equivalent α carbons in the BC, HI and DE loops of VP1 are as large as 5.3, 1.3 and 5.5 Å, respectively, which are statistically significant. The structures of the BC loop of VP1 from P1/Mahoney, P3/Sabin and V510 are shown in Figure 3 and compared in Figure 4.

In a previous comparison of P1/Mahoney with P3/Sabin (Filman *et al.*, 1989), we attempted to identify, in each case, the residues which are responsible for stabilizing the conformation of the BC loop, and the extent to which these residues are conserved within and among each of the three serotypes of poliovirus. The conservation within each serotype of the residues most obviously responsible for stabilizing the conformation of the loop led us to propose that the loop conformation itself might be a conserved attribute of each serotype, and that structural differences in the main chain conformation might well be the basis for serotype-specific immune recognition in poliovirus. The structure of the BC loop in V510 is consistent with these proposals, as it is distinctly different from that observed within either P1/Mahoney or P3/Sabin, and is stabilized by residues conserved among type 2 strains (see below).

Many of the similarities and differences among the three loop structures can be described in terms of two obvious sequence-specific interactions which characterize the loop in V510 and P3/Sabin, but which are absent in P1/Mahoney. These interactions are: (i) a hydrophobic contact on the inner

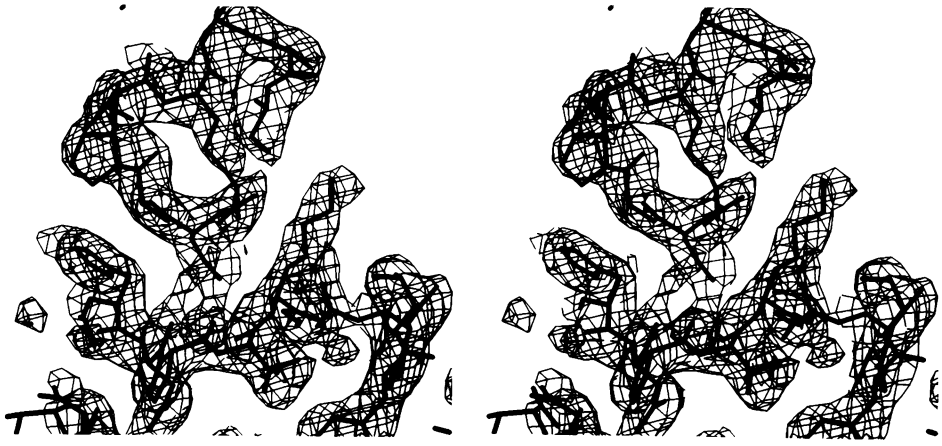

Fig. 2. Icosahedrally-constrained 'omit' electron density in the vicinity of the BC loop of VP1. Initial phases were derived from the Fourier transform of an atomic model from which residues 95–105, 143–152 and 246–252 of VP1 were omitted, and these phases were refined to convergence by iterative application of non-crystallographic symmetry constraints. This figure is a stereo view of a portion of the resulting averaged 'F_0' electron density map, together with corresponding portions of the atomic model. The BC loop (curving clockwise from Asp95 to Ser102) is clearly visible at the top of the figure. The HI loop extends across the center of the figure from His248 (at the left) to Lys252 (at the right). In the lower right of the figure, parts of the DE loop including portions of Phe142, Thr143 and Glu144 are shown. All of the residues omitted in this calculation occupy well-defined continuous electron density at this contour level, except for the side chain amino nitrogen of Lys99 (which is unambiguous at a lower contour level), and the side chains of Arg100 and Asn146 (which are much less well ordered).

surface of the loop between the side chains of Pro97 and Leu104 (Figure 3b and c), and (ii) the presence on the outer surface of the loop of a hydrogen bond between the side chains of the acidic residue at position 95 and the polar residue at position 102 (Figure 3b and c). Although the V510 and P3/Sabin loops are very similar to one another between the β barrel and the site of the hydrophobic contact, the pronounced conformational difference in residues 98–102 appears to be related to the lengths of the side chains which form the hydrogen-bonded 'bridge' across the loop. In most type 3 sequences, residues 95 and 102 are Glu and Gln, respectively (Table III). These large side chains create a fairly long 'bridge' across the loop, and permit a 9.1 Å separation between their respective α carbons. In contrast, type 2 sequences have Asp and Ser residues at these positions (Table III). To accommodate this shorter 'bridge', the main chain at position 102 takes a different course, which results in a separation of only 6.9 Å across the loop, and which shifts the α carbon of Ser102 some 3 Å from its position in P3/Sabin.

Several other sequence-specific interactions also appear to contribute significantly to the stability of the V510 loop conformation (and, in some cases, to differentiate it from types 1 and/or 3). (i) A salt bridge between Asp95 and Lys99 in the V510 is unique to type 2 (Figure 3c). Whereas both residues are conserved among type 2 sequences, none of the known type 1 sequences has an acidic residue at position 95, and all of the known type 3 sequences have a Thr or Ser at position 99 (Table III). (ii) An i-to-i +3 hydrogen bond between residues 96 and 99 of V510 (Figure 3c) [which is also found in P1/Mahoney (Figure 3a) despite differences in sequence and neighboring structure] requires the peptide plane between residues 97 and 98 to be in an orientation that is inconsistent with the formation of a hydrogen bond (in P3/Sabin) between the side oxygen of Gln102 and the main chain nitrogen of Thr98 (Figure 3b). (iii) A hydrogen bond between Lys 252 and Ser102 is unique to V510 (Figure 3c). Although the side chain of Lys252 is conserved and is found in a very similar position and orientation in all three structures, it plays only a peripheral role in stabilizing the BC loop in P3/Sabin, contributing indirectly to neutralizing the charge of Glu95 (Figure 3b), and it has no obvious role in the stabilization of the BC loop in P1/Mahoney.

The BC loop structures exemplify several ways that the replacement of a proline by a non-proline can have a pronounced effect on local structure. Unlike types 2 and 3, P1/Mahoney has a proline at position 95, and lacks a proline at position 97 (Table III). Because the side chain of Pro95 is unable to participate in hydrogen bonding, one obvious consequence of this substitution is the elimination of the 'bridge' between the side chains of residues 95 and 102 which spans the loop in V510 and P3/Sabin. Similarly, proline is incapable of adopting the 'extended' conformation characteristic of the loops in V510 and P3/Sabin. A less predictable consequence of the proline substitutions is the finding that the carboxyl end of the BC loop has a markedly different conformation in P1/Mahoney, even though the sequence of residues 103–105 (Lys/Arg-Leu-Phe) is conserved among all known poliovirus strains (Table III). Thus, in V510 and P3/Sabin, the basic residue at position 103 extends above the loop, Leu104 extends below the loop, and Pro97 folds over the leucine side chain, making favorable hydrophobic contacts (Figure 3b and c). In P1/Mahoney, however, the side chain orientations of residues 103 and 104 are reversed (Figure 3a). Undoubtedly this is due to the elimination of Pro97, and to the steric conflicts between Leu104 and Pro95 which would occur if the type 1 sequence were forced to adopt the type 2 or type 3 conformation. Corresponding to these extensive changes in side chain placement (which we attribute to their interactions with nearby proline residues), we also observe a significant rearrangement of the main chain at positions 103 and 104, together with a realignment of the pair of hydrogen bonds which anchors the base of the BC loop. Thus, a hydrogen bond donated by the amide nitrogen of Asp93 is accepted by the carbonyl oxygen of Lys103 in V510 and P3/Sabin (Figure 3b and c) rather than Leu104 in P1/Mahoney (Figure 3a). Similarly, the hydrogen bond accepted by the side chain

Table II. Statistics for the current V510 atomic model

Resolution no. (Å)[a]	Unique hkl used[b]	% of total shell[c]	R_1 model[d]	R_1 non-x symm.[e]	R_{corr} non-x symm.[f]
∞-14.70	2502	31.5	0.4315	0.1085	0.9656
10.39	5652	40.4	0.3484	0.0782	0.9820
8.49	7387	41.3	0.2803	0.0772	0.9836
7.35	8757	41.6	0.2929	0.0906	0.9760
6.57	9695	40.7	0.2916	0.1028	0.9703
6.00	10535	40.2	0.2643	0.1026	0.9690
5.56	11425	40.2	0.2610	0.1091	0.9660
5.20	12212	40.0	0.2371	0.1067	0.9662
4.90	12982	40.0	0.2160	0.1088	0.9678
4.65	13720	40.0	0.1983	0.1095	0.9660
4.43	14504	40.3	0.1920	0.1118	0.9642
4.24	15245	40.5	0.2027	0.1184	0.9609
4.08	15981	40.8	0.2130	0.1260	0.9559
3.93	16671	40.9	0.2149	0.1366	0.9501
3.80	17276	40.9	0.2303	0.1512	0.9411
3.68	17975	41.2	0.2306	0.1533	0.9382
3.57	18462	41.1	0.2376	0.1619	0.9333
3.46	18819	40.7	0.2607	0.1801	0.9209
3.37	19412	40.8	0.2681	0.1871	0.9116
3.29	19884	40.8	0.2832	0.2024	0.9034
3.21	20248	40.4	0.3053	0.2231	0.8839
3.13	20756	40.5	0.3284	0.2401	0.8692
3.07	20176	38.5	0.3516	0.2660	0.8446
3.00	18459	34.5	0.3759	0.2920	0.8212
2.94	16264	29.8	0.3942	0.3130	0.7968
2.88	14455	25.9	0.3997	0.3256	0.7818
2.83	12811	22.6	0.4524	0.3819	0.7255
2.78	11481	19.9	0.4681	0.4042	0.7000
2.73	10241	17.4	0.4940	0.4298	0.6574
2.68	9046	15.1	0.5010	0.4435	0.6261
2.64	7850	12.9	0.5446	0.4980	0.5605
2.60	6591	11.0	0.5507	0.5735	0.4028
Total	437474	32.8	0.2852	0.1880	0.9208

The current atomic model for V510 includes 6652 non-hydrogen atoms, representing the protein, myristate and palmitate in each protomer, nine atoms corresponding to a planar electron density feature stacked with Trp38 of VP2 (see Filman *et al.*, 1989), and 524 fixed solvent molecules with variable occupancy factors. Resolution-dependent bin scales compensate for overall isotropic thermal motion. The model has a 0.04 Å r.m.s. deviation of the atomic positions from rigidly constrained groups, and a 0.02 Å r.m.s. deviation from standard bond lengths.

[a]The reflections have been divided into 32 shells of roughly equal reciprocal volume. The values in each shell correspond to [b]the number of unique reflections observed and [c]the percentage of theoretically possible reflections which this number represents. R_{corr} (the linear correlation coefficient) and R_1 (the crystallographic 'R-factor') are measures of the agreement between observed and calculated structure factor amplitudes ($|F_{obsd}|$ and $|F_{calc}|$, respectively).

$$R_1 = \frac{\sum_{hkl} ||F_{obsd}| - |F_{calc}||}{\sum_{hkl} |F_{obsd}|}$$

[d]In calculating R_1 (model), F_{calc} is taken to be the Fourier transform of the atomic model. After non-crystallographic symmetry constraints have been applied to model-based phases, the quality of the resulting symmetry-averaged electron density map can be assessed by [e]R_1 (non-x symm.) and [f]R_{corr} (non-x symm.). In calculating these two statistics, F_{calc} is taken to be the Fourier transform of the averaged map.

carboxylate of Asp93 is donated by the amide nitrogen of Lys103 in V510 and P3/Sabin (Figure 3b and c) rather than Leu104 in P1/Mahoney (Figure 3a).

Consistent with our previous observations regarding P3/Sabin and P1/Mahoney, it appears that the side chains which are most obviously involved in stabilizing the BC loop conformation (namely Asp93, Asp95, Pro97, Lys99, Ser102 and Leu104) are highly conserved among type 2 strains (Table III). This suggests that the observed structure is probably typical of type 2 polioviruses, and is consistent with the ability of V510 to elicit and to be neutralized by anti-type 2 antibodies. Potentially, these residues may serve as a 'signature' for the type 2 loop conformation in the classification of other poliovirus sequences, and may facilitate attempts to model the loops computationally by limiting the range of conformational possibilities that it is necessary to sample.

Surprisingly, in the chimera the conformations of both the DE and HI loops are more similar to those observed in P3/Sabin than they are to those observed in the parental P1/Mahoney (Figure 4). In the HI loop, the conformational change is limited to a large movement of the side chain of His248 and smaller adjustments of the main chain of residues 247–250. In both the chimera and P3/Sabin, the position and orientation of the imidazole group of His248 appears to be governed by packing, rather than by specific hydrogen bonding. Steric conflicts would prevent the HI loop of P1/Mahoney from assuming the conformation found in V510

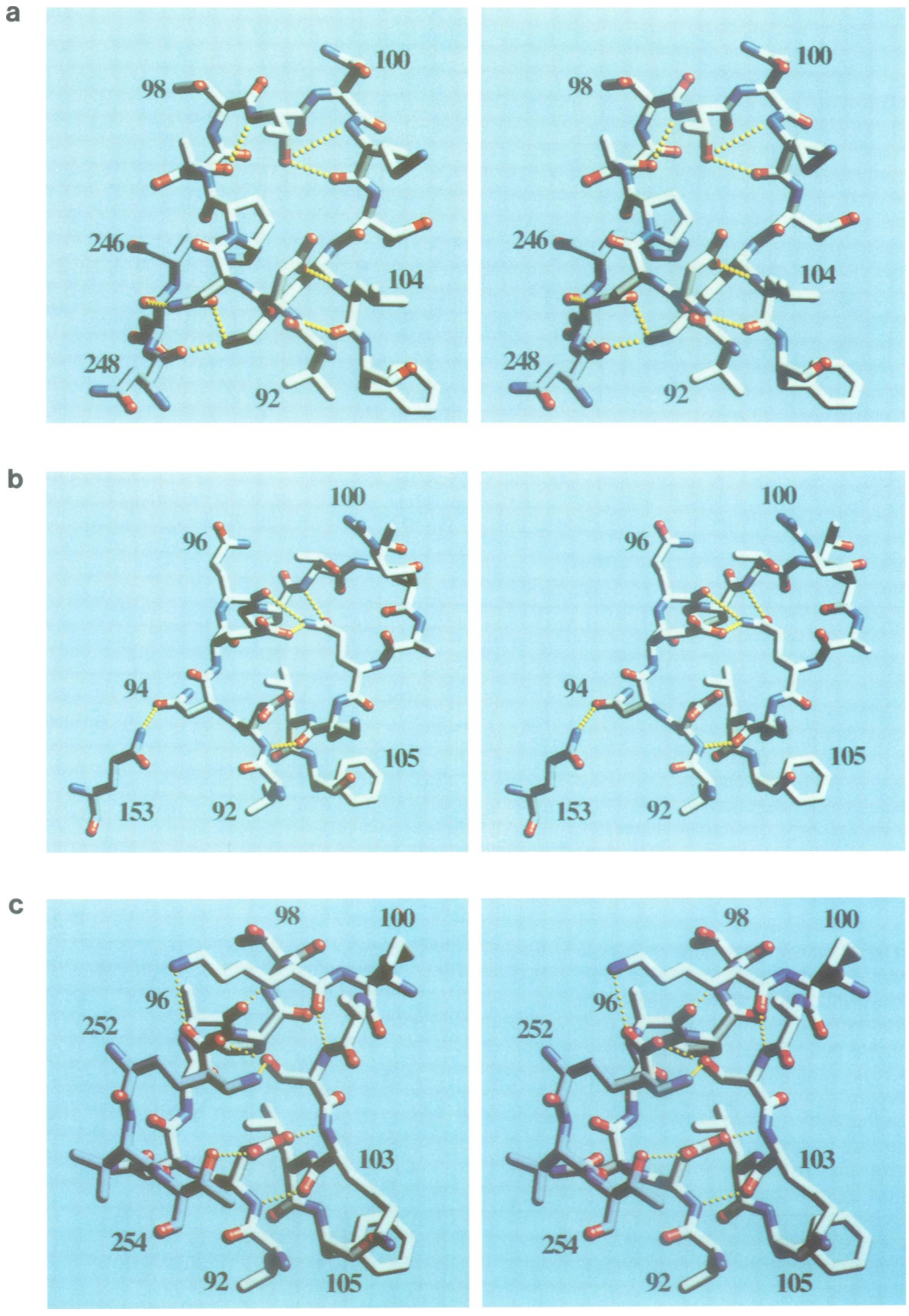

Fig. 3. Atomic models for the BC loops of VP1 of (**a**) P1/Mahoney, (**b**) P3/Sabin and (**c**) V510. In these stereo views, oxygens are red and nitrogens are dark blue. Carbon atoms in the BC loop are shown in white, whereas carbon atoms from neighboring residues which make important stabilizing interactions are colored blue-grey. Yellow dotted lines represent the salt bridges and hydrogen bonds which appear to be important for stabilizing the loop conformations. Selected residue numbers are included as landmarks.

and P3/Sabin, and vice versa. There are no comparable direct interactions which would explain the conformational differences observed in the DE loop. It should be noted, however, that this loop is poorly ordered in all three strains, and it may be that the distribution of allowed structures in the loop are correlated with the structure of the nearby BC loop.

Structural differences distant from the replaced loop

Other than the loops of VP1 clustered around the five-fold axes, icosahedrally averaged difference maps have shown only two other locations in which V510 differs significantly from P1/Mahoney. First, V510 appears to have a cation bound to the outer surface of capsid protein VP3, tetrahedrally co-ordinated by the side chains of His97, Glu102

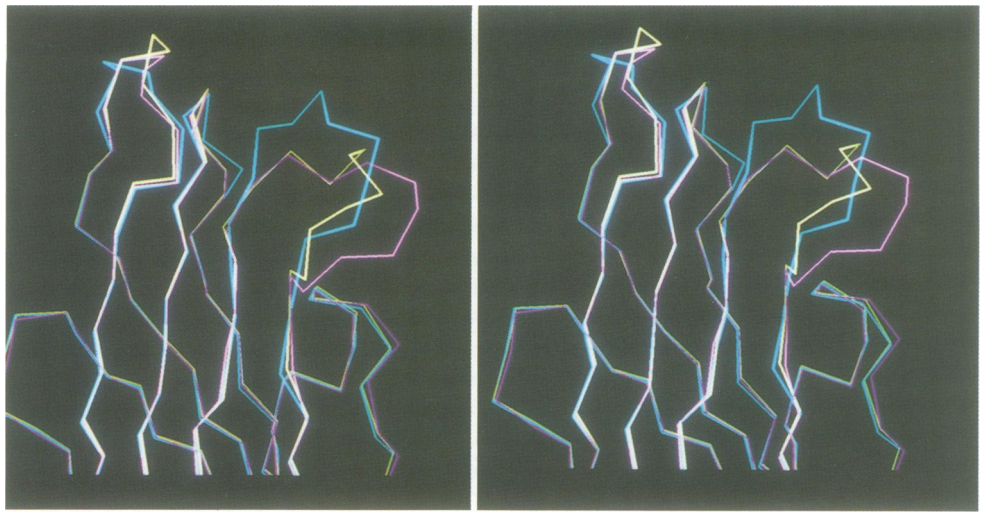

Fig. 4. Superimposed α carbon models showing the narrow end of the VP1 β barrel in P1/Mahoney (cyan), V510 (yellow) and P3/Sabin (magenta). In this stereo view, the outer surface of the virus is towards the right and in the front. The FG, DE, HI, BC and EF loops are shown clockwise from left to right. The three poliovirus structures clearly are very similar, except in portions of the DE, HI and BC loops.

Table III. Consensus sequences for the BC loop of VP1 in poliovirus[a]

	Residue no.														
	91	92	93	94	95	96	97	98	99	100	101	102	103	104	105
Type 1 (11)	Thr	Val	Asp	Asn	Ser	Ala	Ser	Thr	Thr	Ser	Lys	Asp	Lys	Leu	Phe
Type 2 (13)	Glu	Val	Asp	Asn	Asp	Ala	Pro	Thr	Lys	Arg	Ala	Ser	Lys	Leu	Phe
Type 3 (13)	Glu	Val	Asp	Asn	Glu	Gln	Pro	Thr	Thr	Arg	Ala	Gln	Lys	Leu	Phe
Overall	–	Val	Asp	Asn	–	–	–	Thr	–	–	–	–	Lys	Leu	Phe

[a]The consensus sequences are based on sequence information from 11 strains of type 1 poliovirus, 13 strains of type 2 poliovirus and 13 strains of type 3 poliovirus. For type 1 and type 3 poliovirus the underlined residues indicate positions where there are two or more substitutions in the known strains. For type 2, two of the 13 sequences differ at amino acid 103 (underlined), which is a Lys in the Lansing strain and an Arg in the Sabin strain. The sequence of P1/Mahoney is identical to the type 1 consensus sequence, except at positions 95 (which is Pro) and at 100 (which is Asn). The sequence of P3/Sabin is identical to the type 3 consensus sequence. Adapted from Minor *et al.* (1987).

and His230. In P1/Mahoney, these side chains are arranged in a similar way, but the cation is replaced by a water molecule. We surmise that this difference is due to the inclusion of EDTA in the purification of P1/Mahoney, but not of V510. Quite possibly, the cation is Zn^{2+}, considering both its apparent co-ordination, and that both V510 and P1/Mahoney are crystallized in the presence of millimolar levels of Ca^{2+} and Mg^{2+}. The conservation (in all known poliovirus sequences) of the side chains which form the cation site, and the apparent ion specificity of the site both suggest that the bound ion might play a specific biological role at some stage of the viral life cycle.

The second difference in ligand binding occurs in the hydrophobic center of the β barrel of VP1. This site has been shown to bind a variety of hydrophobic molecules, including a number of antiviral drugs which inhibit the uncoating of rhinovirus (Smith *et al.*, 1986; Badger *et al.*, 1988) and poliovirus (Grant,R.A., Filman,D.J., Jow,L., Lockshin,C., Andries,K. and Hogle,J.M., manuscript in preparation). In every poliovirus structure solved to date, the center of the VP1 β barrel has been occupied by an elongated electron density feature which appears to be a 16-carbon saturated aliphatic chain. The 15 most deeply buried atoms in the chain interact exclusively with hydrophobic side chains from the core of VP1 and from the amino terminus of VP3. Beyond the 15th carbon, the binding pocket is polar, and the ligand usually is less well ordered.

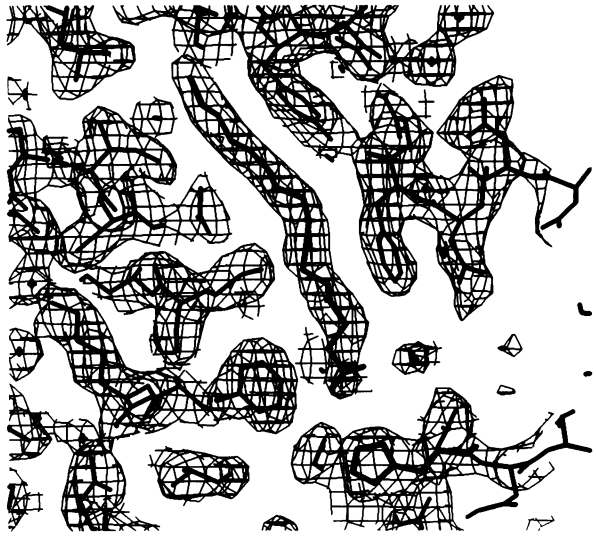

Fig. 5. Symmetry-averaged electron density in the vicinity of the ligand which occupies the hydrophobic core of VP1 in V510. Portions of the atomic model are shown. The ligand (which has been modeled as palmitate in V510) extends from top to bottom. At the top of the figure, the hydrocarbon tail of the fatty acid interacts exclusively with hydrophobic side chains of VP1. At the bottom of the figure, the polar head group of the ligand is a predominantly hydrophilic environment close to the outer surface of the virion. As modeled, the carboxylate group of palmitate is hydrogen bonded with the imidazole group of His207 of VP1 (bottom right).

In both P1/Mahoney and P3/Sabin, the shape of the electron density feature and the nature of its interactions with the protein are consistent with a tentative identification of the ligand as sphingosine (Filman *et al.*, 1989). In V510, however, the density follows a different course at the 13th aliphatic carbon (Figure 5). Rather than turning towards the outer surface of the particle, the density feature follows a straight course from the 8th carbon through the 16th, heading directly towards the imidazole side chain of His207. The density feature terminates abruptly at the 17th atom, which appears to be hydrogen bonded to the imidazole group, and which we surmise is a terminal oxygen from the carboxylate group of a palmitic acid molecule.

In light of the conservation of His207 in all known poliovirus structures (but not in other picornaviruses), the near perfect complementarity between palmitate and its binding site, the significant degree of order in its polar head group, and the obvious inability of any larger molecule to bind in this orientation, it is almost surprising that an electron density feature resembling palmitate has been observed on only one other occasion. Among the other poliovirus structures currently being solved in our laboratory (native-antigenic empty capsids and a variety of P1/Mahoney and P3/Sabin mutants), the apparent identity of the substituent has been variable. The appearance of the electron density feature does not seem to correlate with the strain of the virus, the method of purification of the virus, or the cell line on which it grows. Our observation that the density for the polar head group is generally less well ordered than the hydrophobic portion may be indicative that the site is occupied by a mixture of lipids.

Discussion

Implications for the molecular mechanism of mouse-adaptation

In principle, the inability of a particular virus to grow successfully in a specific host, tissue or cell might be attributable to the inability of the virus to carry out any of the steps in its replicative cycle. Thus, host-specific restriction might involve cell attachment, entry, uncoating, genome replication, translation, assembly or cell lysis. In addressing the determinants of mouse-adaptation in poliovirus, however, only the early steps in infection (attachment, entry and uncoating) need be considered because the ability of poliovirus to replicate in mouse cells upon transfection with viral RNA has been well documented (Holland *et al.*, 1959).

The importance of the viral capsid as a determinant of mouse-adaptation in P2/Lansing was first established by the demonstration that recombinant viruses in which the entire capsid coding region of P1/Mahoney was replaced with that of P2/Lansing were mouse-virulent (La Monica *et al.*, 1986). The subsequent finding that variants of P2/Lansing (selected for resistance to type 2-specific monoclonal antibodies and having mutations in the BC loop of VP1) were attenuated in mice (La Monica *et al.*, 1987) suggested that important determinants of mouse virulence might be located in the BC loop. Finally, the virulence of the V510 chimera (Martin *et al.*, 1988) and of a similar chimera reported by Murray *et al.* (1988a) established the BC loop of P2/Lansing alone was sufficient to render P1/Mahoney mouse-adapted. In this context, the structure of V510 provides an excellent opportunity to study the specific structural features of the infectious virion which are responsible for mouse-virulence, to identify the early event in infection which is sensitive to these features, and ultimately to provide an explanation at the molecular level for mouse-adaptation.

The crystal structure of V510 clearly shows that the six sequence changes in the BC loop which render the mouse-avirulent P1/Mahoney strain mouse-adapted also have a pronounced effect on the conformation of the loop itself. This raises the question of whether the loop conformation is in itself an important determinant of host tropism, either directly, or by way of its effect on neighboring structures. If the loop conformation is important, we would expect the 'signature' residues which stabilize the loop conformation to have a significant influence on mouse-adaptation. This prediction is consistent with the results of studies which have examined the effects of mutations in the BC loop produced by site-directed mutagenesis (Martin *et al.*, 1991; Moss and Racaniello, 1991) and by the selection of variants which are resistant to neutralization by site 1-specific anti-type 2 monoclonal antibodies (La Monica *et al.*, 1987; Couderc *et al.*, 1991). These studies have shown that substitutions at Asp93, Asp95 or Leu104 result in decreased viability and loss of mouse virulence, and that substitutions at Pro97, Lys99 or Ser102 produce significant attenuation of the variants in mice.

When the structures of the mouse-adapted V510 and the mouse-avirulent P1/Mahoney are compared (Figure 6), it is apparent that pronounced differences in shape, charge distribution and solvent accessibility occur in a localized region of the virion surface in the vicinity of the particle five-fold axis. Furthermore, when the residues which have been shown to be important for mouse virulence in V510 (La Monica *et al.*, 1987; Couderc *et al.*, 1991; Martin *et al.*, 1991; Moss and Racaniello, 1991) or P2/Lansing (Ren *et al.*, 1991) are mapped to the structure of the virion, together with the sequence differences which differentiate the mouse-adapted LSa strain of type 1 poliovirus from its mouse-avirulent parent, P1/Mahoney (O.Kew, personal communication), it is apparent that the residues critical for mouse virulence are located in a very tight cluster at the apex of the five-fold peak (Figure 6d).

The simplest explanation for the importance of highly exposed portions of the viral capsid in regulating mouse-adaptation is that mouse-virulence is determined by the ability of the virus to attach to a specific receptor in the mouse central nervous system. An alternative, but less straightforward possibility is that mouse-adaptation is determined by the ability of the virion to undergo conformational changes which are required for cell entry or uncoating subsequent to receptor attachment. The gene for the HeLa cell poliovirus receptor has recently been cloned and sequenced (Mendelsohn *et al.*, 1989). Evidence supporting the idea that the 'defect' in P1/Mahoney replication in mice operates at the level of receptor interaction (or receptor-mediated conformational change) is provided by the observation that cultured mouse cells (which normally are resistant to poliovirus infection) become susceptible when transfected with the cloned gene for the HeLa cell receptor (Mendelsohn *et al.*, 1986, 1989). Moreover, transgenic mice which express the HeLa cell receptor can be infected with primate-specific strains of poliovirus resulting in paralytic poliomyelitis (Ren *et al.*, 1990).

If mouse-adaptation in V510 and P2/Lansing is, in fact, determined at the level of receptor interaction, the

importance of the highly exposed BC loop and the clustering of significant structural and chemical changes in the chimera suggest that the mouse receptor interacts with a site near the particle five-fold axis. This model would imply that a significant component of the binding site for the endogenous mouse receptor is located in a highly exposed surface feature, and is part of a well characterized antigenic site. This is inconsistent with the 'canyon hypothesis' of Rossmann which predicts that residues critical for receptor binding should be inaccessible to antibodies (Rossmann *et al.*, 1985; Rossmann, 1989), but is analogous to receptor binding by foot-and-mouth disease virus, which is believed to involve a highly exposed loop (the GH loop of VP1) in the immediate vicinity of another neutralizing antigenic site (Acharya *et al.*, 1989).

Direct participation of the BC loop of VP1 in binding to the receptor in the mouse central nervous system would imply fundamental differences in between the determinants of receptor binding in the mouse central nervous system and

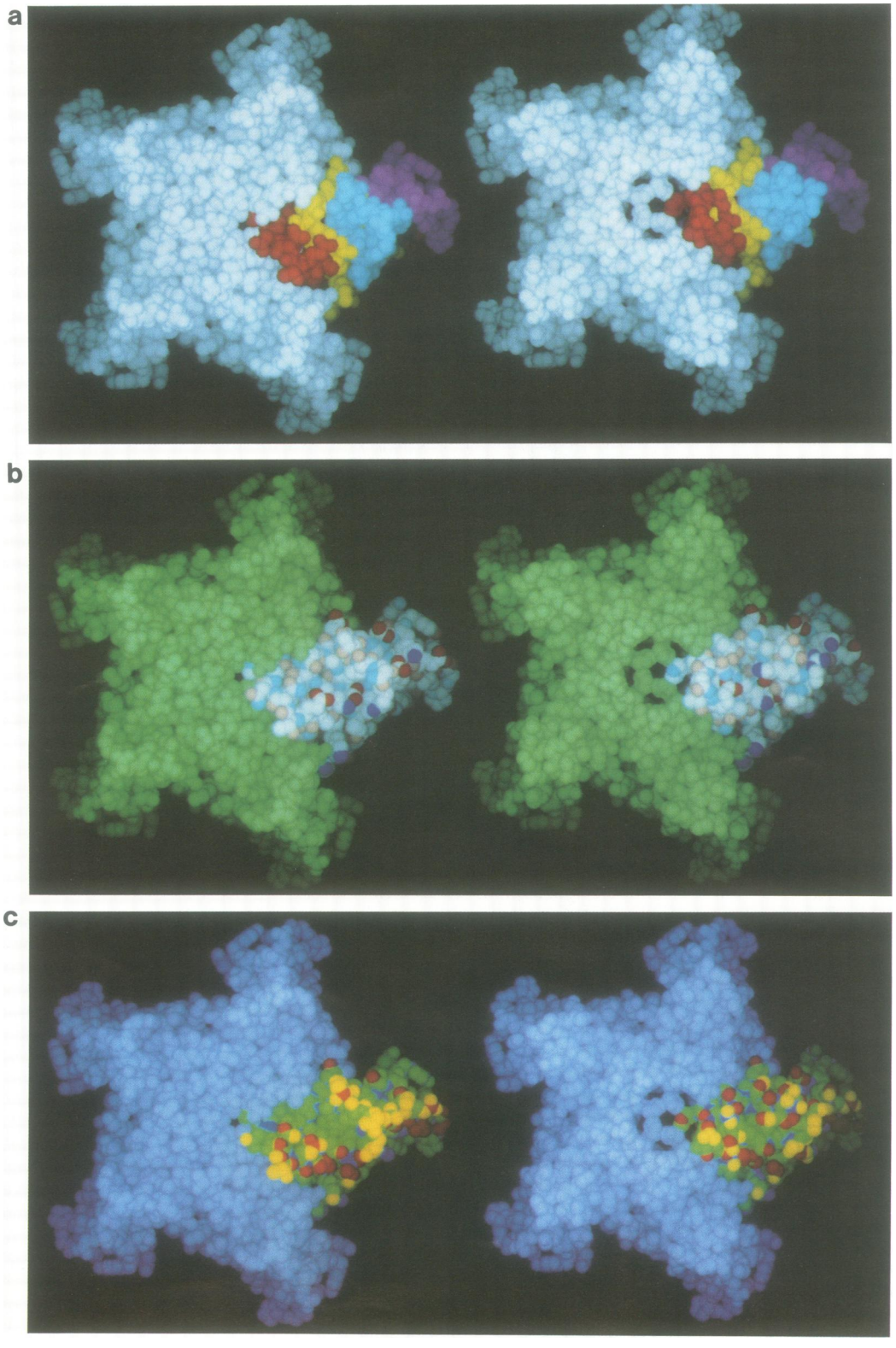

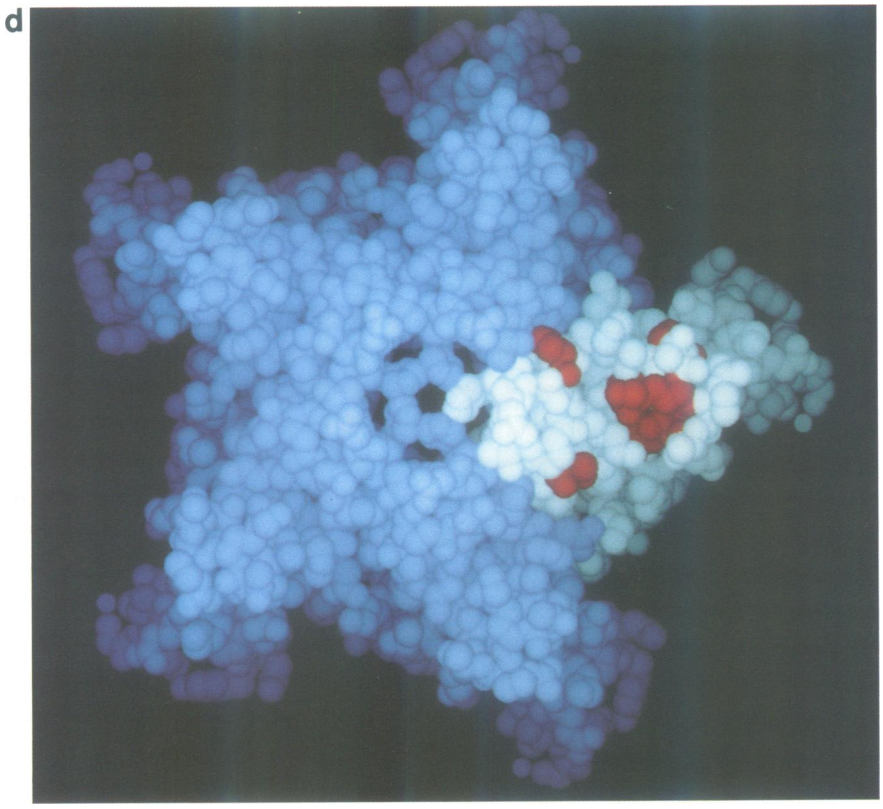

Fig. 6. Space-filling atomic models of the outer surface of poliovirus in the vicinity of the five-fold axis. In panels a–c P1/Mahoney is on the left and V510 is on the right. Panel **a** shows the locations of the DE (red), HI (yellow), BC (cyan) and EF (magenta) loops of VP1 in a reference protomer. Panel **b** shows the distribution of charged atoms on the surface of the reference protomer. Full and partial positive charges are dark and light blue respectively. Full and partial negative charges are red and pink respectively. In panel **c** each atom is colored according to its accessibility to spherical probes of various radii. The least exposed atoms (dark blue) are inaccessible to 5 Å probes. Atoms accessible by 5, 10 and 20 Å probes are shown in green, red and yellow, respectively. Note that the replacement of the BC loop (and associated conformational differences) produces a substantial change in the shape of the outer surface in the vicinity of the five-fold axis. In V510, the BC and DE loops are displaced outward, away from the five-fold axis, relative to their positions in P1/Mahoney. As a result, V510 has better delineated prominences at the periphery of the 'mesa' which dominates the surface at the five-fold axis, and a well-defined hole at the five-fold axis itself, which exposes the side chain of His149. Replacement of the BC loop also produces significant changes in the detailed chemical properties of the surface. Thus, V510 has fewer exposed negative charges and a greater number of exposed positive charges than P1/Mahoney (panel b). In addition, V510 lacks the ridge of highly exposed residues which is formed by the BC loop in P1/Mahoney. In P1/Mahoney this ridge significantly reduces the exposure of the neighboring HI and DE loops, relative to V510 (panel c). In panel **d** residues known to regulate the mouse-virulence of poliovirus are shown in the context of the structure of V510. These critical side chains (which are indicated in red) cluster at the top of the large radial projection ('mesa') at the five-fold axis.

in cultured primate cells, since several lines of evidence suggest that the BC loop is not a primary determinant of poliovirus infectivity in primate cells. Thus, there is minimal loss of infectivity when the BC loop of VP1 is cleaved with trypsin (Fricks *et al.*, 1985), replaced by extraneous (non-poliovirus) sequences in chimeric viruses (Burke *et al.*, 1988; Colbere-Garapin *et al.*, 1988; Martin *et al.*, 1988; Murray *et al.*, 1988a,b; Evans *et al.*, 1989; Murdin and Wimmer, 1989; Jenkins *et al.*, 1990), or deleted entirely (Girard *et al.*, 1990). Furthermore, the BC loop is a site of considerable sequence diversity among the three serotypes of poliovirus [which are known to compete for the same receptor in cultured cells (Crowell, 1966)], and is the site of the greatest structural differences between P1/Mahoney and P3/Sabin (Filman *et al.*, 1989).

The importance of exposed residues near the five-fold axis for receptor binding in mice, but not in primate cells, could be explained in several ways: (i) the receptor responsible for binding mouse-adapted viruses in the mouse central nervous system may be a homolog of the primate receptor, but differences between the primate and murine receptors may result in an expansion of the binding site on the virus for the murine receptor to include residues near the five-fold axis. A homolog of the HeLa cell receptor is expressed in a variety of mouse cells and tissues (Racaniello, 1990). (ii) The murine receptor may be less efficient at inducing the conformational changes in the virus which are required for cell entry and viral uncoating. Structural changes in the vicinity of the five-fold axes might compensate for this inefficiency by making the receptor-induced conformational changes more energetically favorable. (iii) The functional receptor in the mouse may involve additional proteins which are responsible for the sensitivity to changes in the vicinity of the five-fold axis. (iv) The murine receptor which is responsible for binding mouse-adapted viruses may be entirely unrelated to the HeLa cell receptor.

Interestingly, despite the strong evidence for the role of the HeLa cell receptor described by Mendelsohn *et al.* (1989), there is evidence that a second receptor or receptor component may be expressed in human cells. Shepley *et al.* have described a protein from HeLa cells which elicits antibodies that inhibit poliovirus infection in a serotype-specific fashion (blocking infection with type 1 and type 2 but not type 3 polioviruses) (Shepley *et al.*, 1988). Such serotype specificity is consistent with the involvement of antigenic sites in receptor binding. Moreover, unlike the

primary HeLa cell receptor [which is expressed in a wide variety of tissues (Mendelsohn *et al.*, 1989; Freistadt *et al.*, 1990)], this 'second receptor' is expressed preferentially by tissues which support poliovirus replication in natural infection (Shepley *et al.*, 1988). Thus, the role of this protein as a second receptor or receptor component could explain the tissue specificity of poliovirus infection in primates. The apparent sensitivity of this 'second receptor' to the structures of antigenic sites, together with its preferential expression in the central nervous system, are reminiscent of the properties of poliovirus infection in mice. This suggests that a homologous protein in the mouse may be responsible for supporting poliovirus replication.

Unfortunately, the molecular mechanism for mouse-adaptation has proved to be a difficult question to address experimentally because P2/Lansing and V510 infect mice only by direct introduction into the mouse central nervous system, and because neither strain infects common murine cell lines in culture. Therefore, many of the questions which have been raised still remain unresolved. However, as outlined above, the structure of the V510 chimera provides powerful constraints on the alternative models. We expect that the availability of the V510 structure will prove useful in the design and interpretation of future studies of the viral and receptor-linked determinants of host range and tissue tropism.

Materials and methods

Crystallization and data collection

The construction and characterization of the V510 chimera has been described elsewhere (Martin *et al.*, 1988). Low-passage seed stocks of V510 were propagated in HeLa cells in suspension and purified by differential centrifugation and CsCl density gradient fractionation as described previously (Rueckert and Pallansch, 1981). Purified virus was pelleted and resuspended at 10 mg/ml in 0.25 M NaCl in PMC7 buffer (10 mM PIPES, 5 mM $MgCl_2$, 1 mM $CaCl_2$, pH 7.0). The virus was crystallized by microdialysis versus progressively lower concentrations of NaCl in PMC7 at 4°C. Crystals generally appeared at ~0.1 M NaCl. Prior to data collection the crystals were transferred to 25% (v/v) ethylene glycol in PMC7 and mounted in quartz capillaries. The crystals are nearly isomorphous with those of P1/Mahoney (space group $P2_12_12$ with a = 323.3 Å, b = 358.5 Å, c = 380.5 Å and with 0.5 virus particle per asymmetric unit). The crystals diffract at least to 2.6 Å resolution. Three-dimensional diffraction data were collected at −15°C by oscillation photography (25′ of arc per photograph), using an Enraf-Nonius GX-18 rotating anode generator (operated at 40 kV, 55 mA, with a 100 μ focus and Franks mirror optics). The films were digitized on a 50 μ raster, the crystal orientation determined by auto-indexing (T.O.Yeates and D.J.Filman, unpublished) and the data integrated and processed as described previously (Filman *et al.*, 1989).

Structure determination and refinement

The structure was determined by molecular replacement based on the refined model of P1/Mahoney (Hogle *et al.*, 1985; Filman *et al.*, 1989). The orientation and position of the virus particle in the $P2_12_12$ cell is dictated by packing considerations (requiring the crystallographic c axis to coincide with one of the icosahedral two-fold axes of the virus), except for two degrees of freedom (which correspond to a rotation of the particle about this axis, and a translation along it). The orientation and position of the particle (together with the V510 cell parameters) were optimized by trials. In each trial, symmetry averaged P1/Mahoney electron density was positioned in the V510 cell according to the parameter values, and the transform of the resulting map was compared with the V510 data set. The refined position and orientation (corresponding to a fractional translation of −0.2497 along, and a rotation of 2.23 degrees about the c axis) are not significantly different from those observed in P1/Mahoney. Phases for the V510 data were calculated from an appropriately positioned refined model of P1/Mahoney. In the initial phase calculation, residues 94−102 of VP1, ordered solvent and a lipid molecule bound in the center of the VP1 β barrel were omitted from the phasing model. These preliminary phases were refined by the application of 30-fold non-crystallographic symmetry constraints (Bricogne, 1974). After seven cycles of symmetry averaging, the maps were of sufficient quality to build the correct structure for the omitted residues of VP1. Significant structural differences were confirmed and model-built using icosahedrally-constrained omit maps and difference maps (Figure 2). The resulting model was refined using alternating cycles of stereochemically-constrained pseudo-real space atomic refinement (Filman *et al.*, 1989), non-crystallographic averaging and interactive model building. In the pseudo-real space refinement procedure, atomic positional shifts are derived by local evaluation of the gradient of a map calculated by Fourier inversion of the 'vector' difference ($\Delta A + i\Delta B$), after resolution-dependent scaling, between the transforms of 'averaged' and 'model-based' electron densities, each evaluated over an arbitrary volume sufficient to enclose one protomer. Subsequently, a stereochemically-restrained atomic model is derived from these shifted atomic positions by using them as 'targets' for the rigid-body superposition of multiple overlapping constrained chemical groups. This method has also been used to refine the structures of P1/Mahoney and P3/Sabin (Filman *et al.*, 1989).

Acknowledgements

The authors would like to thank Drs Vincent Racaniello, Eric Moss and Olen Kew for helpful discussions and for sharing their data with us prior to publication. This is publication number 6951-MB from the Research Institute of Scripps Clinic. This work was supported by Public Health Service Grant no. AI20566 (to J.M.H.) and T32 NS07078 (to T.O.Y.).

References

Acharya,R., Fry,E., Stuart,D., Fox,G., Rowlands,D. and Brown,F. (1989) *Nature*, **337**, 709−716.
Badger,J. *et al.* (1988) *Proc. Natl. Acad. Sci. USA*, **85**, 3304−3308.
Bricogne,G. (1974) *Acta Crystallogr.*, **A30**, 395−405.
Burke,K.L., Dunn,G., Ferguson,M., Minor,P.D. and Almond,J.W. (1988) *Nature*, **332**, 81−82.
Colbere-Garapin,F., Christodoulou,C., Crainic,R, Garapin,A.-C. and Candrea,A. (1988) *Proc. Natl. Acad. Sci. USA*, **85**, 8668−8672.
Couderc,T., Martin,A., Wychowski,C., Girard,M., Horaud,F. and Crainic,R. (1991) *J. Gen. Virol.*, **72**, 973−977.
Crowell,R.L. (1966) *J. Bacteriol.*, **91**, 198−204.
Evans,D.J., McKeating,J., Meredith,J.M., Burke,K.L., Katrak,K., John,A., Ferguson,M., Minor,P.D., Weiss,R.A. and Almond,J.W. (1989) *Nature*, **339**, 385−388.
Filman,D.J., Syed,R., Chow,M., Macadam,A.J., Minor,P.D. and Hogle,J.M. (1989) *EMBO J.*, **8**, 1567−1579.
Freistadt,M.S., Kaplan,G. and Racaniello,V.R. (1990) *Mol. Cell. Biol.*, **10**, 5700−5706.
Fricks,C., Icenogle,J. and Hogle,J.M. (1985) *J. Virol.*, **54**, 856−859.
Girard,M., Marc,D., Martin,A., Couderc,T., Benichou,D., Candrea,A., Crainic,R., Horaud,F. and van der Werf,S. (1990) In Brinton,M.A. and Heinz,S.X. (eds), *New Aspects of Positive-Strand RNA Viruses*. American Society for Microbiology, Washington, DC, pp. 319−327.
Hogle,J.M., Chow,M. and Filman,D.J. (1985) *Science*, **229**, 1358−1365.
Holland,J.J., McLaren,J.C. and Syverton,J.T. (1959) *J. Exp. Med.*, **110**, 65−80.
Jenkins,O., Cason,J., Burke,K.L., Lunney,D., Gillen,A., Patel,D., McCance,D.J. and Almond,J.W. (1990) *J. Virol.*, **64**, 1201−1206.
Kim,S., Smith,T.J., Chapman,M.S., Rossmann,M.G., Pevear,D.C., Dutko,F.J., Felock,P.J., Diana,G.D. and McKinlay,M.A. (1989) *J. Mol. Biol.*, **210**, 91−111.
La Monica,N., Meriam,C. and Racaniello,V.R. (1986) *J. Virol.*, **57**, 515−525.
La Monica,N, Kupsky,W.J. and Racaniello,V.R. (1987) *Virology*, **161**, 429−437.
Luo,M., Vriend,G., Kamer,G., Minor,I., Arnold,E., Rossmann,M.G., Boege,U., Scraba,D.G., Duke,G.M. and Palmenberg,A.C. (1987) *Science*, **235**, 182−191.
Martin,A., Wychowski,C., Couderc,T., Crainic,R., Hogle,J. and Girard,M. (1988) *EMBO J.*, **7**, 2839−2847.
Martin,A., Benichou,D., Couderc,T., Hogle,J.M., Wychowski,C., van der Werf,S. and Girard,M. (1991) *Virology*, **180**, 648−658.
Mendelsohn,C., Johnson,B., Lionetti,K.A., Nobis,P., Wimmer,E. and Racaniello,V.R. (1986) *Proc. Natl. Acad. Sci. USA*, **83**, 7845−7849.
Mendelsohn,C.L., Wimmer.E. and Racaniello,V.R. (1989) *Cell*, **56**, 855−865.
Minor,P.D., Ferguson,M., Evans,D.M.A. and Icenogle,J.P. (1986) *J. Virol.*, **67**, 1283−1291.

Minor,P.D., Ferguson,M., Phillips,A., McGrath,D.I., Huovilainen,A. and Hovi,T. (1987) *J. Gen. Virol.*, **68**, 1857–1865.
Moss,E.G. and Racaniello,V.R. (1991) *EMBO J.*, **10**, 1067–1074.
Murdin,A.D. and Wimmer,E. (1989) *J. Virol.*, **63**, 5251–5257.
Murray,M.G., Bradley,J., Yang,X.-F., Wimmer,E., Moss,E.G. and Racaniello,V.R. (1988a) *Science*, **241**, 213–215.
Murray,M.G., Kuhn,R.J., Arita,M., Kawamura,N., Nomoto,A. and Wimmer,E. (1988b) *Proc. Natl. Acad. Sci. USA*, **85**, 3203–3207.
Page,G.S., Mosser,A.G., Hogle,J.M., Filman,D.J., Rueckert,R.R. and Chow,M. (1988) *J. Virol.*, **62**, 1781–1794.
Racaniello,V.R. (1990) *Curr. Top. Microbiol. Immunol.*, **161**, 1–22.
Ren,R., Costantini,F., Gorgacz,E.J., Lee,J.J. and Racaniello,V.R. (1990) *Cell*, **63**, 353–362.
Ren,R., Moss,E.G. and Racaniello,V.R. (1991) *J. Virol.*, **65**, 1377–1382.
Rossmann,M.G. (1989) *J. Biol. Chem.*, **264**, 14587–14590.
Rossmann,M.G. *et al.* (1985) *Nature*, **317**, 145–153.
Rueckert,R.R. and Pallansch,M.A. (1981) *Methods Enzymol.*, **78**, 315–325.
Shepley,M.P., Sherry,B. and Weiner,H.L. (1988) *Proc. Natl. Acad. Sci. USA*, **85**, 7743–7747.
Smith,T.J., Kremer,M.J., Luo,M., Vriend,G., Arnold,E., Kamer,G., Rossmann,M.G., McKinlay,M.A., Diana,G.D. and Otto,M.J. (1986) *Science*, **233**, 1286–1293.

Received on March 18, 1991; revised on May 14, 1991